FREEZE-THAW CHARACTERISTICS OF AGGREGATES

by
Geo. R. Laughlin, Research Engineer
John W. Scott, Research Engineer
and
Jas. H. Havens, Director of Research

DEPARTMENT OF HIGHWAYS
Commonwealth of Kentucky

Prepared for the 16th Annual
Highway Geology Symposium,
University of Kentucky, March
25-27, 1965

INTRODUCTION

Premature deterioration of concrete under freezing and thawing conditions is often attributable to the aggregate fraction. Past research has shown that the freeze-thaw characteristics of aggregate are related, in a general way, to such properties as: 1) porosity, 2) absorption, and 3) bulk specific gravity. Actually it is the pore system--that is, the size, shape, arrangement and continuity of the pores--that governs the freeze-thaw characteristics. Distress in aggregate particles arises from hydrostatic pressure induced when a portion of its absorbed pore-water is frozen. The degree of distress or damage manifested is dependent upon the amount of permeable porosity, the degree of saturation, the severity of freezing, and the rupture strength of the rock particle and the restraint imposed upon it.

Porosity, an index to the pore system, is expressed as the ratio of the void or pore volume to the total volume. Absorption, an index to the pore system, is expressed as a ratio of the weight of absorbed water to the weight of the solid component. Since this ratio is dependent upon the specific gravity of the solid component, it may be quite variable. Bulk specific gravity, another index to the pore system, is also quite variable since it is dependent upon the specific gravity of the solid component. It is evident, of course, that porosity is an independent parameter. If absorption, which is

easily determined, were expressed as the ratio of volume of water to the total bulk volume of the rock particle, then this index would also be independent of other parameters.

The exact limits that should be placed on these physical properties to control aggregate quality remains controversial. This is due not only to the variables just mentioned but also to the methods used for determining aggregate durability. Present methods employ composite samples for tests; and, therefore, the results of such tests are composite or average values. For example, the average value of absorption obtained from a composite sample may exhibit a low value--indicating a sound aggregate; however, if each particle were analyzed, it might be found that a portion of the aggregate is so highly absorptive as to be detrimental to concrete. It is the percentage of these deleterious particles in aggregate that is so important.

A second factor in freeze-thaw testing is the antecedent moisture condition of the aggregate--which heretofore has not been duly considered. For instance, a sample of aggregate which is in a highly saturated condition in its natural environment or a stockpile may be oven-dried in preparation for laboratory freeze-thaw testing; many of the standard procedures require that this be done routinely. Even subsequent re-soaking often fails to restore the original

moisture condition; and, since aggregate must be critically saturated to be vulnerable to damage, the duration of such freeze-thaw testing may merely reflect the time required for the aggregate to become critically saturated. Ideally, in such testing, consideration should be given to: 1) from a given antecedent moisture condition, the time required for the aggregate to acquire critical saturation in the environment to be imposed and, 2) once critically saturated, whether the aggregate can withstand the stresses accompanying freezing.

Heretofore, the discrete conditions previously mentioned have not been compensated for by methods of test in determining aggregate soundness. Logically, in determining the soundness of an aggregate sample, the freeze-thaw testing should be conducted on a per particle basis. Each particle should be saturated at the onset of test and kept saturated during testing. For study purposes the degree of saturation may be varied. However, maximum saturation definitely establishes the ultimate susceptibility of aggregate to damage from freezing and thawing.

In order to obtain objective data pertaining to the freeze-thaw characteristics of aggregate--that is, to establish more definitive relationships between the effects of freezing and thawing of an aggregate and its physical properties of

porosity, absorption and bulk specific gravity--a method of test was devised whereby the discrete conditions previously mentioned were fulfilled. A freezing medium was sought, whereby each particle could be frozen quickly. By doing this, the quickly frozen surface would form a seal or shell about the particle and thus retain the pore water. Also, the medium should not contaminate the pore water. Chilled mercury was chosen as the freezing medium--it has high thermal conductivity; it is nonmiscible with water; and it has a low freezing-point. The test consisted of submerging the aggregate particle in the prechilled mercury. From preliminary testing, it was found that if a particle did not show visual distress at the end of four cycles--which could be performed in a matter of minutes--it would withstand innumerable cycles. For analysis, it was desired to have a saturated gravel which would represent a variety of rock types and possess a wide range of physical properties. To meet these conditions, a sample was secured from a glacial outwash deposit and kept inundated.

MATERIALS AND PROCEDURES

The primary constituents of the aggregate sample were dolomites, cherts, limestones, sandstones, siltstones, and various igneous and metamorphic rock particles. Although usually acceptable for concrete, this gravel contained both sound and unsound particles and, thereby, provided an assortment of particles needed for the study.

The sample was graded into the following sieve sizes:

Passing 1-1/2-inch and retained on 1-inch,
Passing 1-inch and retained on 3/4-inch,
Passing 3/4-inch and retained on 1/2-inch,
Passing 1/2-inch and retained on 3/8-inch, and
Passing 3/8-inch and retained on No. 4.

After grading according to size, each particle was numbered. The saturated surface-dry weight and bulk volume were obtained for each particle prior to the freeze-and-thaw tests. The weight was obtained by weighing each surface-dry particle in a capsule, and the volume was obtained by weighing the amount of mercury displacement.

Calculations for the bulk specific gravity were made for each particle by the use of the following expression:

$$G_{SSD} = \frac{W_T \gamma_M}{W_M \gamma_W}$$

where:

G_{SSD} = bulk specific gravity (saturated surface-dry),
W_T = saturated surface-dry weight of particle,
γ_M = density of mercury at temperature of test,
W_M = weight of mercury displaced by particle, and
γ_W = density of water at temperature of test.

The freezing of the aggregate was accomplished by submerging each particle in cold mercury (-30°C to -35°C) for a period of five minutes. The freezing apparatus is shown in Figure 1. The mercury was contained in a glass cylinder enclosed in an insulated container of dry ice (solid CO_2). A low-temperature thermometer was used to observe the temperature of the mercury.

At the end of each freezing cycle, each particle was removed from the freezing medium and returned to a container of water and allowed to thaw. At the end of each thawing cycle, a visual examination was made of each particle; and any distress resulting from the freezing and thawing cycle was recorded.

For obvious reasons the absorptive values for each particle were not determined until the conclusion of freeze-and-thaw testing. Also, since any losses due to chipping and spalling would vary the weight of the particle, the saturated surface-dry weight of each particle (or major pieces thereof) was

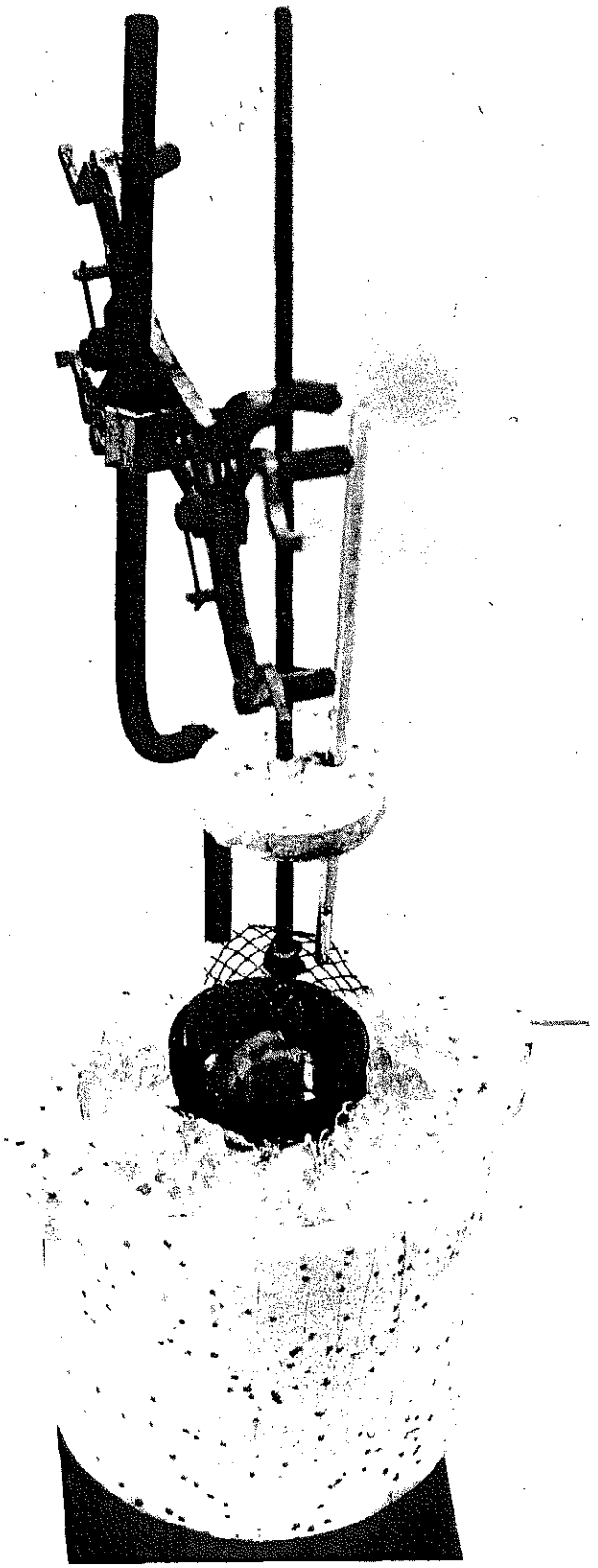

Figure 1: Freezing Apparatus.

determined for the second time. Each particle (or major piece) was then dried (110°C) to a constant weight.

Calculations for the absorption of each particle were made by the use of the following expression:

$$\omega = \frac{W_T - W_S}{W_S} \times 100$$

where:

ω = absorption expressed as a per cent,

W_T = saturated surface-dry weight of particle (or major pieces), and

W_S = oven-dry weight of particle (or major pieces).

Porosity calculations were made by the use of the following expression for saturated aggregate:

$$\eta = \frac{\omega}{100 + \omega} G_{SSD} \times 100$$

where:

η = porosity expressed as a per cent,

ω = absorption expressed as a per cent, and

G_{SSD} = bulk specific gravity (saturated surface-dry).

It should be emphasized that the above equation applies only for saturated aggregate.

After all other testing was completed, a fresh surface of each particle was examined by use of binocular and petrographic microscopes. Where necessary, the petrographic examination was supplemented by chemical tests. Mineralogical and textural features were recorded.

RESULTS

The accumulated number of fractured particles at the end of each freeze-thaw cycle, expressed as a percentage of the total number of particles, is presented graphically in Figure 2. The slope of the curve indicates the increase in the percentage of fractured particles at the end of each cycle; and, as would be expected, the largest increase occurred at the end of the first cycle. Of the total number fractured, approximately 70 per cent occurred during the first freezing cycle. The small increases in the accumulated percentage of fractured particles which occurred with succeeding cycles are probably due to the fact that many of the particles had undetected fractures at the end of the first freezing cycle and additional cycles were needed before the fractures became visible. The condition of the particles at the end of the fourth cycle of freeze-and-thaw testing was used for correlation.

The percentage of fractured particles at the end of the fourth cycle of freeze-and-thaw, for each particle size tested, is given in Figure 3. The largest percentage of fractured particles occurred in the 1/2-inch size; whereas, the smallest percentage of fractured particles occurred in the 1-inch and No. 4 sizes. The average percentage of fractured particles in all sizes combined is indicated by the

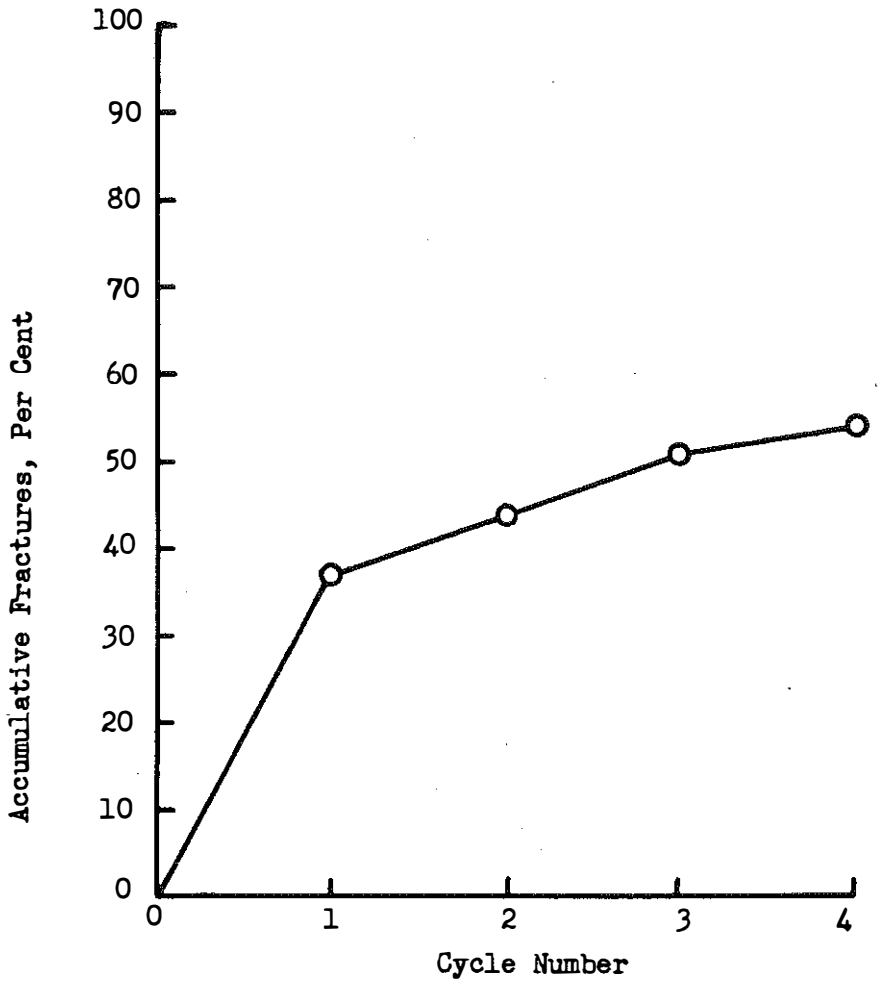

Figure 2: Accumulative Percentage of Fractured Particles for Each Cycle of Freeze-and-Thaw.

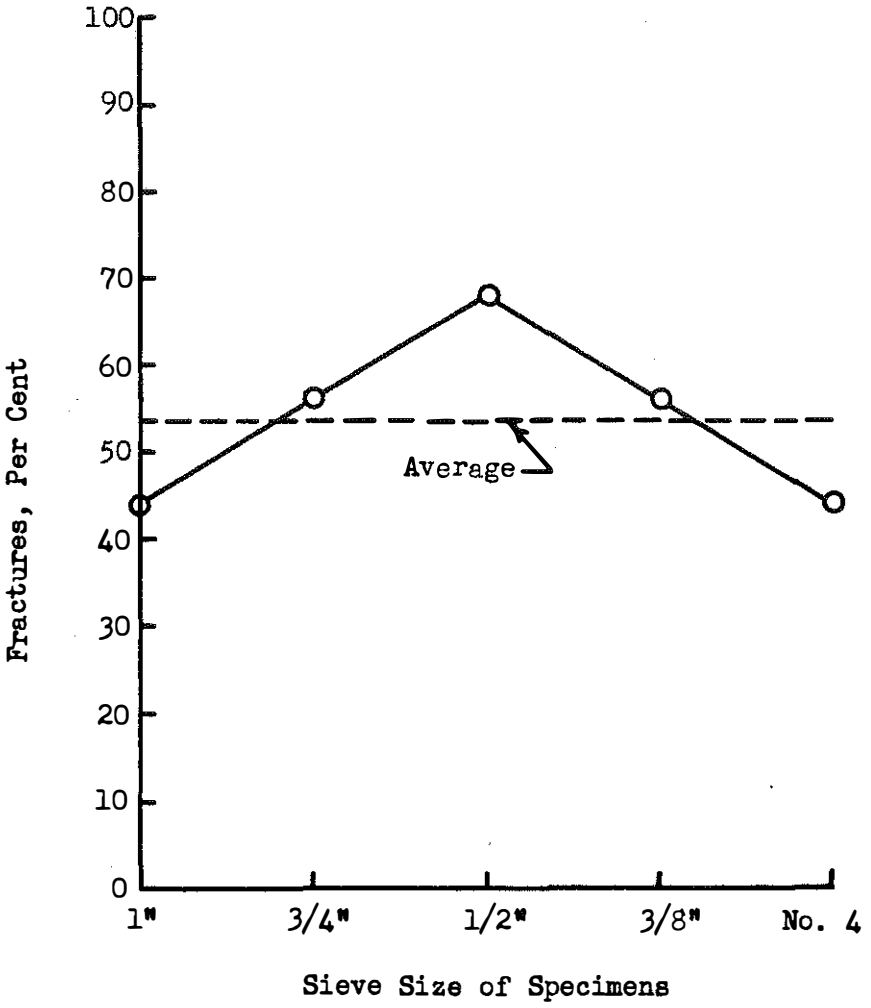

Figure 3: Relationship between Particle Size and Percentage of Fractured Particles after Exposure to 4 Cycles of Freeze-and-Thaw.

dashed line, at 53.6 per cent. The 1-inch size particles consisted mostly of igneous and metamorphic rock particles which, by their mode of formation, are less porous than the water-lain sedimentary rocks. The bulk of the 1/2-inch particles consisted of porous cherts and porous dolomites. The bulk of the No. 4 size particles were mostly quartz.

The relationship between the soundness of the test particles and their adjusted porosity values is shown in Figure 4. As expected, particles in the higher porosity range were less durable than particles of the lower range. All particles having a porosity of more than 11 per cent fractured; whereas, less than 25 per cent of the particles having a porosity of less than 2 per cent fractured.

A graph depicting the relationship between the percentage of fractured particles and the absorption values of the test particles is shown in Figure 5. All particles having absorptions of 4 per cent or greater failed when subjected to freezing and thawing. However, very few specimens having absorptions of less than 1 per cent failed. Between these extremes, the percentage of particles failing increased as the absorption increased.

The percentage of fractured particles at the end of 4 cycles of freeze-and-thaw for different bulk specific gravity

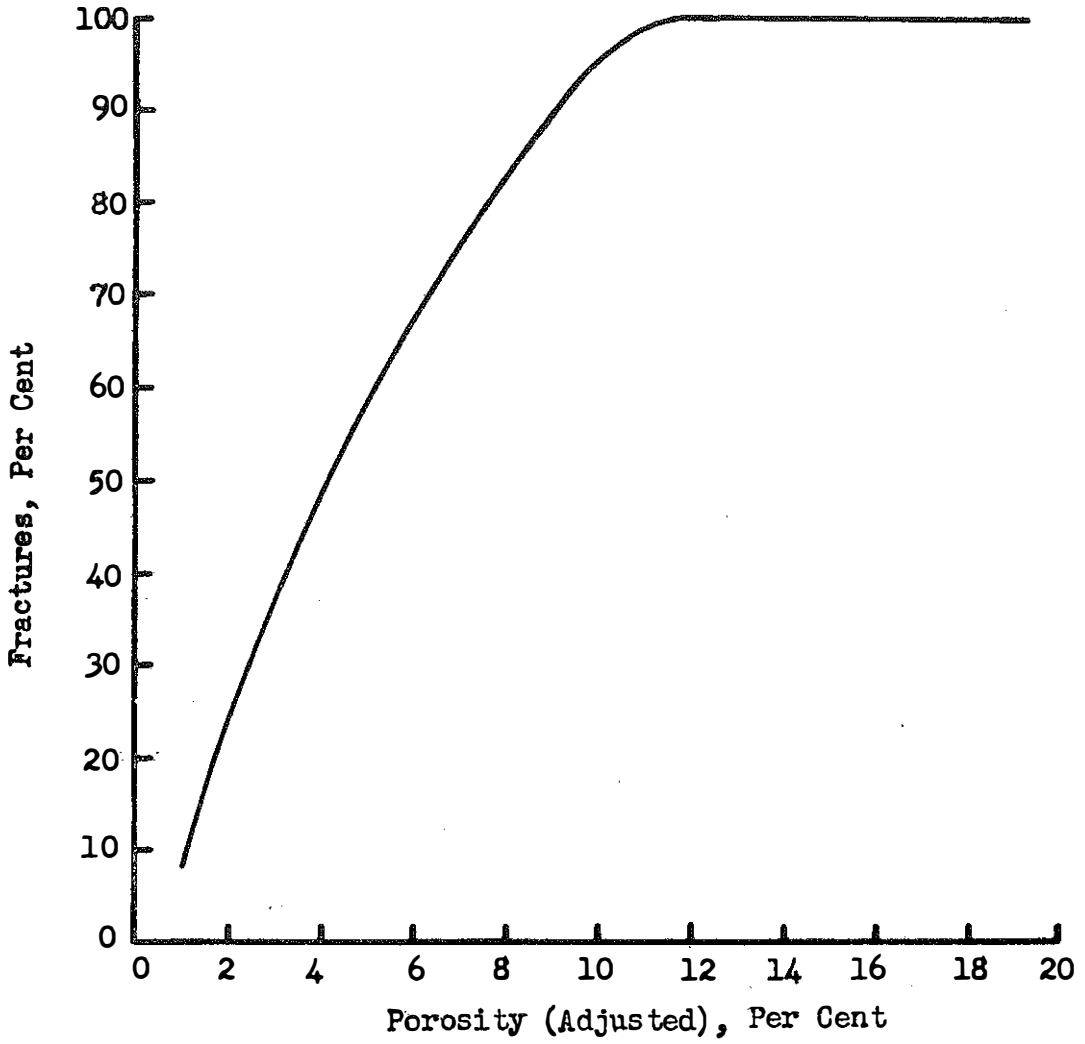

Figure 4: Relationship between Porosity (Adjusted Value) and Percentage of Fractured Particles after Exposure to 4 Cycles of Freeze-and-Thaw.

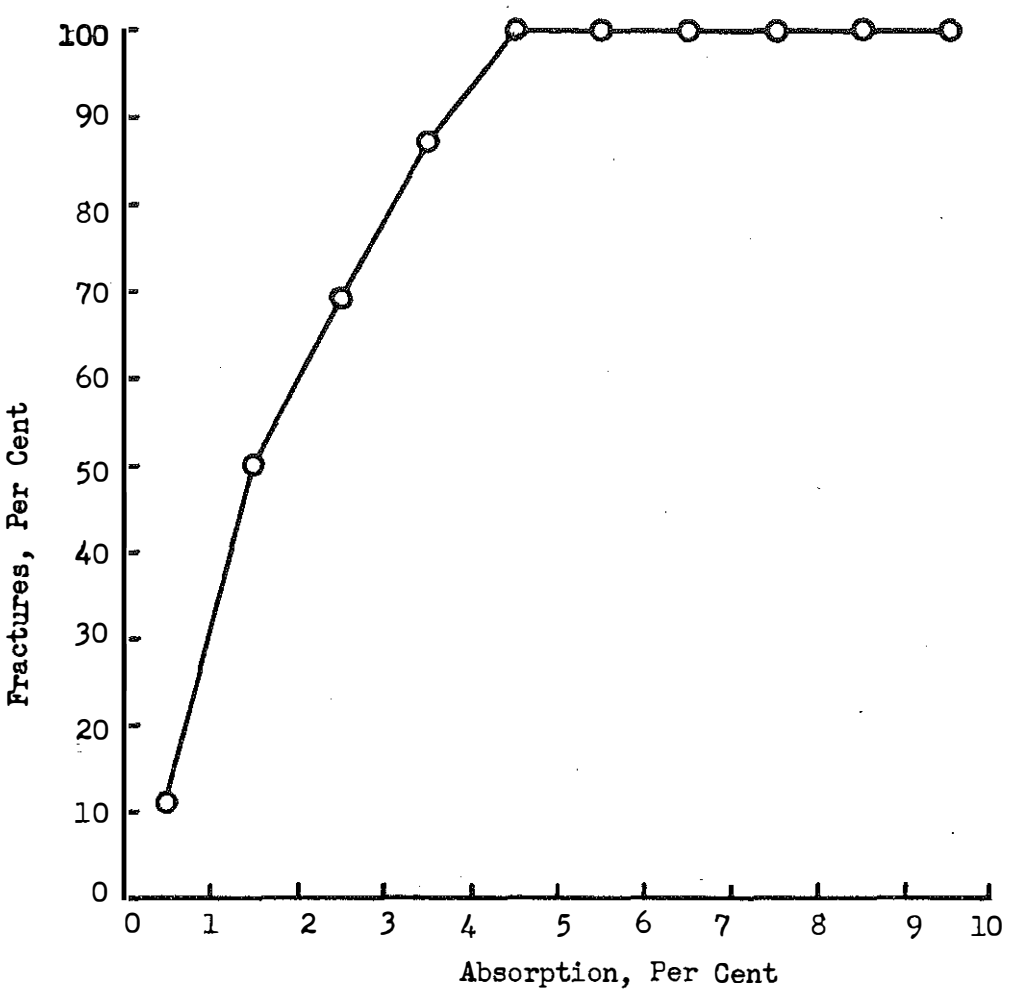

Figure 5: Relationship between Absorption and Percentage of Fractured Particles after Exposure to 4 Cycles of Freeze-and-Thaw.

values is shown in Figure 6. A definite trend is established, indicating that aggregate in the lower specific gravity ranges has lower resistance to freezing and thawing than aggregate of the higher specific gravity ranges. However, no specific gravity level can be classed as critical--except the level below 2.40. The increase in fractured particles in the heavier bulk specific gravity range is due to highly porous, highly absorptive dolomites. For comparison, suggested curves for cherts and dolomites are included.

The durability of the various types of aggregate particles is presented in Table 1. Sedimentary rock particles had a much larger percentage of fractures than the igneous and metamorphic particles. Within the sedimentary classification, limestone contained the least percentage of fractured particles, whereas dolomite contained the greatest.

It is interesting to note that chert, which is usually thought of as being very unsound under freeze-and-thaw action, did not have the greatest percentage of fractured particles. Since porous, absorptive chert and porous, absorptive dolomites may be similar in appearance, it is possible that, in the past, some concrete deteriorations which were thought to be due to unsound chert were, in reality, due to unsound dolomite.

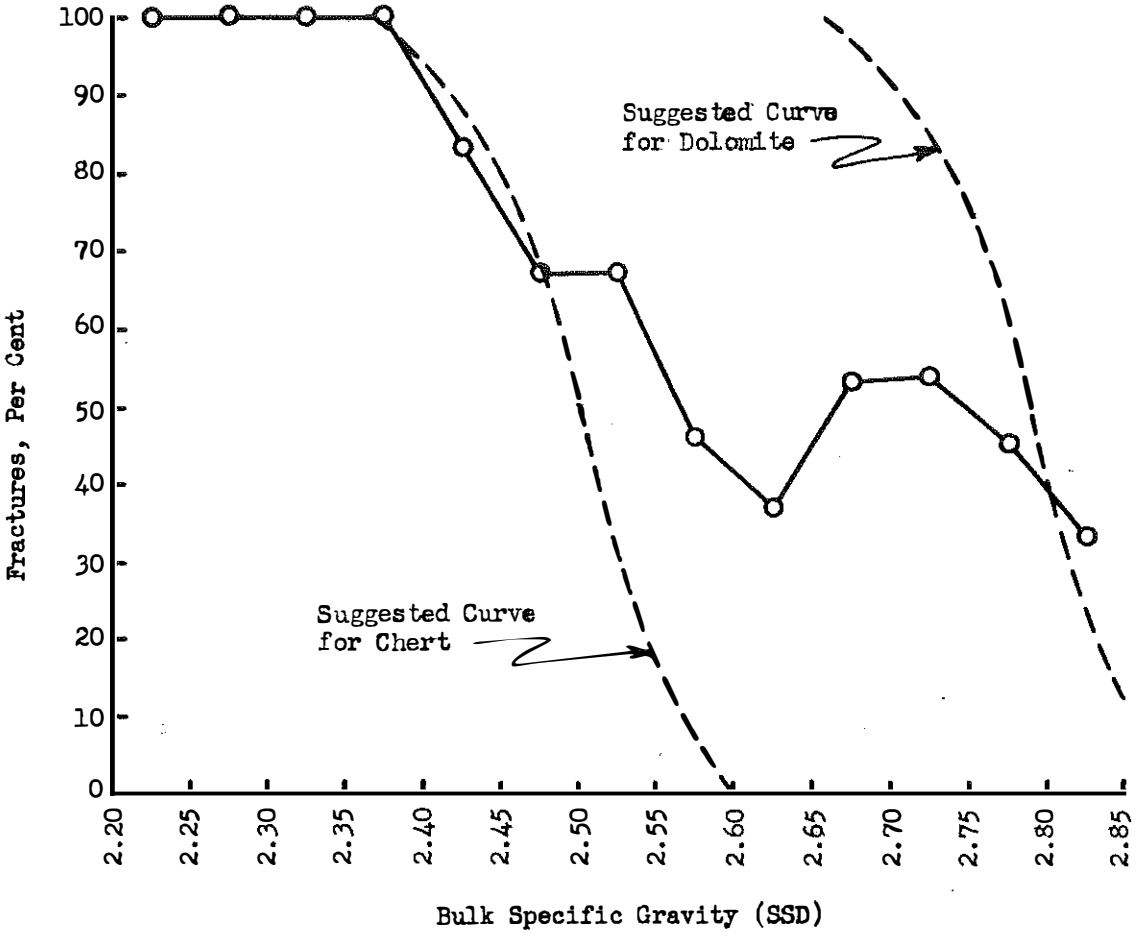

Figure 6: Relationship between Bulk Specific Gravity (Saturated Surface-Dry Condition) and Percentage of Fractured Particles after Exposure to 4 Cycles of Freeze-and-Thaw.

TABLE 1

DURABILITY OF AGGREGATE ACCORDING TO CLASSIFICATION

Classification	Per Cent Fractured Particles at End of 4 Cycles of Freeze-and-Thaw
1) Sedimentary	66
a) Dolomite	77
b) Chert	59
c) Limestone	41
d) Sandstone & Siltstone	69
2) Igneous and Metamorphic	23

DISCUSSION

Porosity, Absorption and Bulk Specific Gravity

Figure 4 and Figure 5, depicting relationships between porosity and per cent fractured particles and between absorption and per cent fractured particles are similar. This is because calculations were based on a two-phase system--i.e., water and solids. This being the case, porosity may be related directly to absorption. With a given porosity and assuming that all voids permeable, the corresponding saturated absorption value may be computed by assuming a value for apparent specific gravity. Figure 7 shows such a relationship. These absorption values were calculated by taking the specific gravity of the solid components to be 2.65 and 2.94.

If critical porosity is taken to be two per cent, critical absorption could range from 0.695 for chert having a specific gravity of 2.65; to 0.77 for dolomite having a specific gravity of 2.94.

Bulk specific gravity and its apparent relationship to the percentage of fractured particles may or may not reflect the true durability of an aggregate. Even though all natural aggregate having bulk specific gravities below 2.40 are normally considered to be deleterious, aggregates in the

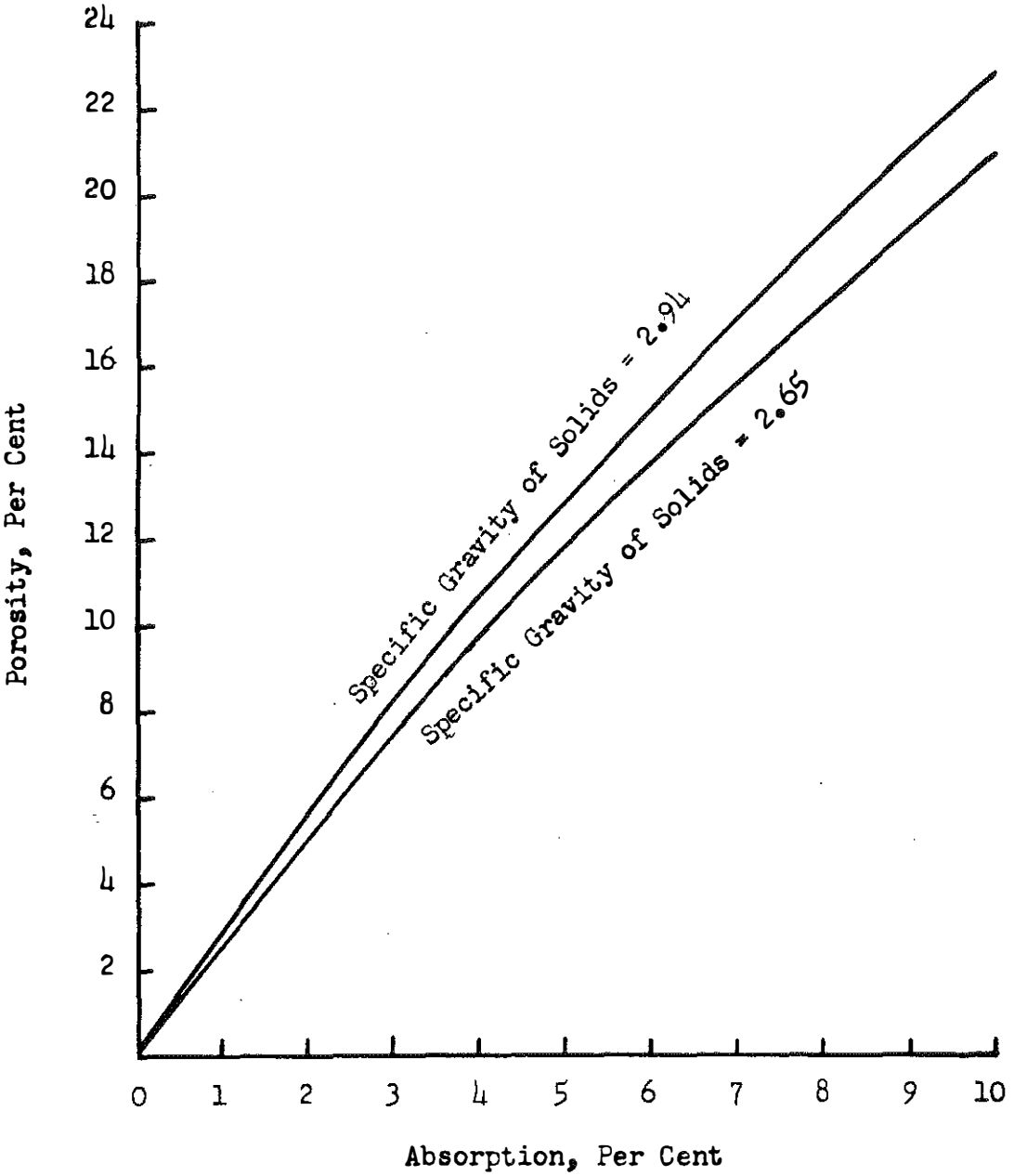

Figure 7: Theoretical Relationship between Porosity and Absorption when all Pores are Permeable and Saturated.

heavy bulk specific gravity ranges may be just as deleterious. This is well illustrated by the dolomites shown in Figure 6. Moreover, in quarrying a limestone deposit which has a large proportion of granoblastic dolomite facies, the bulk specific gravity of the highly porous, highly absorptive dolomite would correspond with the bulk specific gravity of the high quality limestone facies.

Theoretical Considerations of Freezing Effects

The ability of a rock fragment to withstand internal pressures accompanying freezing is controlled by certain inherent properties of the fragment. Insight into these properties is gained through Timoshenko's (23) explanation of Lamé's solution for the radial and tangential normal stresses in a thick-walled, spherical container under internal and external pressures is considered (Figure 8). According to Timoshenko, the radial normal stress is given by the expression:

$$\sigma_R = \frac{P_o b^3 (R^3 - a^3)}{R^3 (a^3 - b^3)} + \frac{P_i a^3 (b^3 - R^3)}{R^3 (a^3 - b^3)}$$

and the tangential normal stress is obtained by the equation:

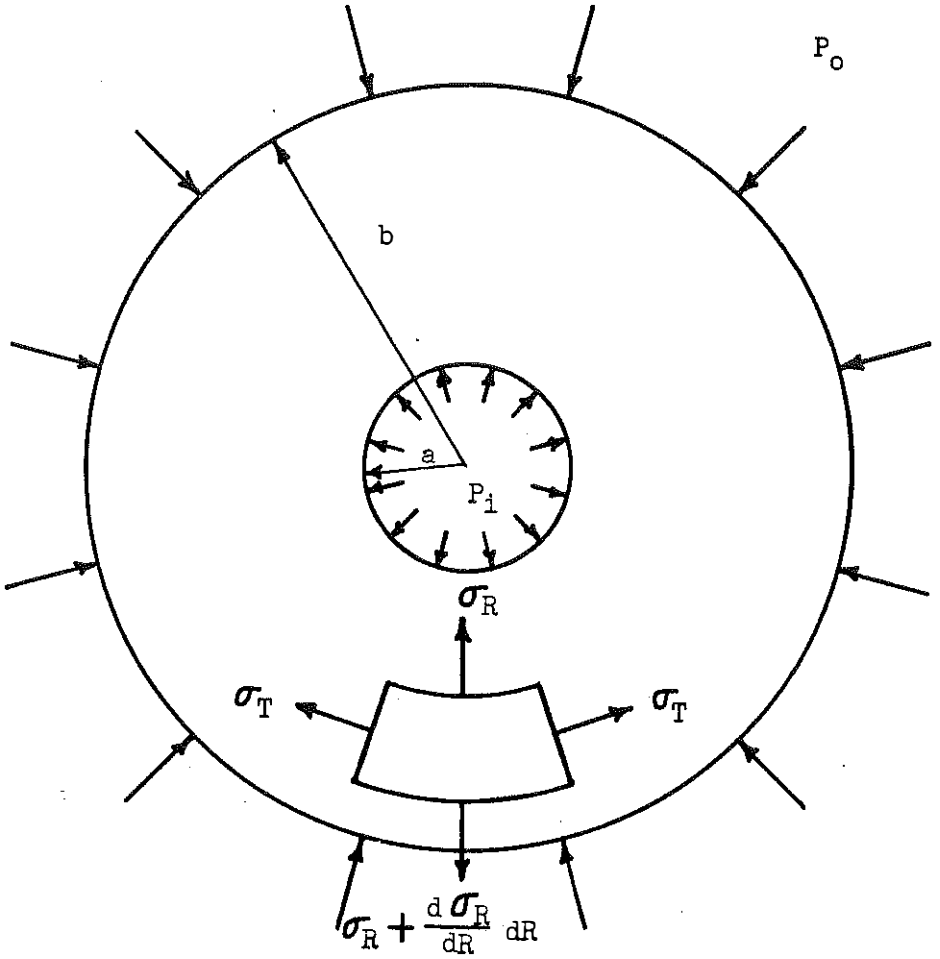

Figure 8: Thick-Walled Sphere under Internal and External Pressures (cf. Reference 23).

$$\sigma_T = \frac{P_o b^3 (2R^3 + a^3)}{2R^3 (a^3 - b^3)} - \frac{P_i a^3 (2R^3 + b^3)}{2R^3 (a^3 - b^3)}$$

where:

a = inner radius of the sphere,

b = outer radius of the sphere,

P_i = the internal pressure, and

P_o = the external pressure.

If the exterior confining pressure (P_o) is zero, the equations for the normal stresses at the extreme outer fiber are as follows:

$$\sigma_R = 0$$

$$\sigma_T = - \frac{3P_i a^3}{2 (a^3 - b^3)}$$

and by multiplying and dividing the latter equation by $4/3\ \pi$ and substituting:

$V_v = 4/3\ \pi\ a^3$,

$V_t = 4/3\ \pi\ b^3$, and

$V_v = \eta\ V_t$

where:

V_v = volume of voids,

V_t = volume of sphere, and

η = porosity as defined above,

the equation reduces to

$$\sigma_T = 3/2\ P_i \frac{\eta}{1 - \eta}$$

The radial normal stress, σ_R, along the outer edge of the spherical container is zero and the tangential normal stress, σ_T, at the same point, which is a tensile stress, is dependent upon the porosity and the internal pressure created. Conversely, the ability of a spherical container to withstand a given internal pressure is dependent upon the porosity and tensile strength of the container and is independent of size or total volume.

If the tensile strength, σ_u, is inserted in the above equation for σ_T, the equation becomes

$$P_u = 2/3\ \sigma_u \frac{(1 - \eta)}{\eta}$$

where:

P_u = maximum allowable internal pressure, and

σ_u = tensile strength.

Tensile strengths of the gravel particles were not determined, but similar materials have tensile strengths ranging

from 100 to 1000 psi (8). With a known tensile strength, the maximum allowable internal pressure for various porosity values may be calculated. Three porosity-pressure curves for tensile strengths of 300, 600, and 900 psi are shown in Figure 9.

The determination of the internal pressure accompanying freezing of water within a hollow sphere may, likewise, be approached for a theoretical standpoint. If the temperature-volume changes of the sphere, water, and ice are neglected, the volume of ice within the cavity, assuming all the water freezes, is as follows:

$$V_i = 4/3\ \pi\ a^3 S(1+\beta)(1-\frac{P_a}{K})$$

where:

V_i = volume of ice,

S = degree of saturation,

β = volume increase accompanying freezing of water,

P_a = available internal pressure, and

K = bulk modulus of ice.

The tangential strain at any point within the sphere is given by the expression:

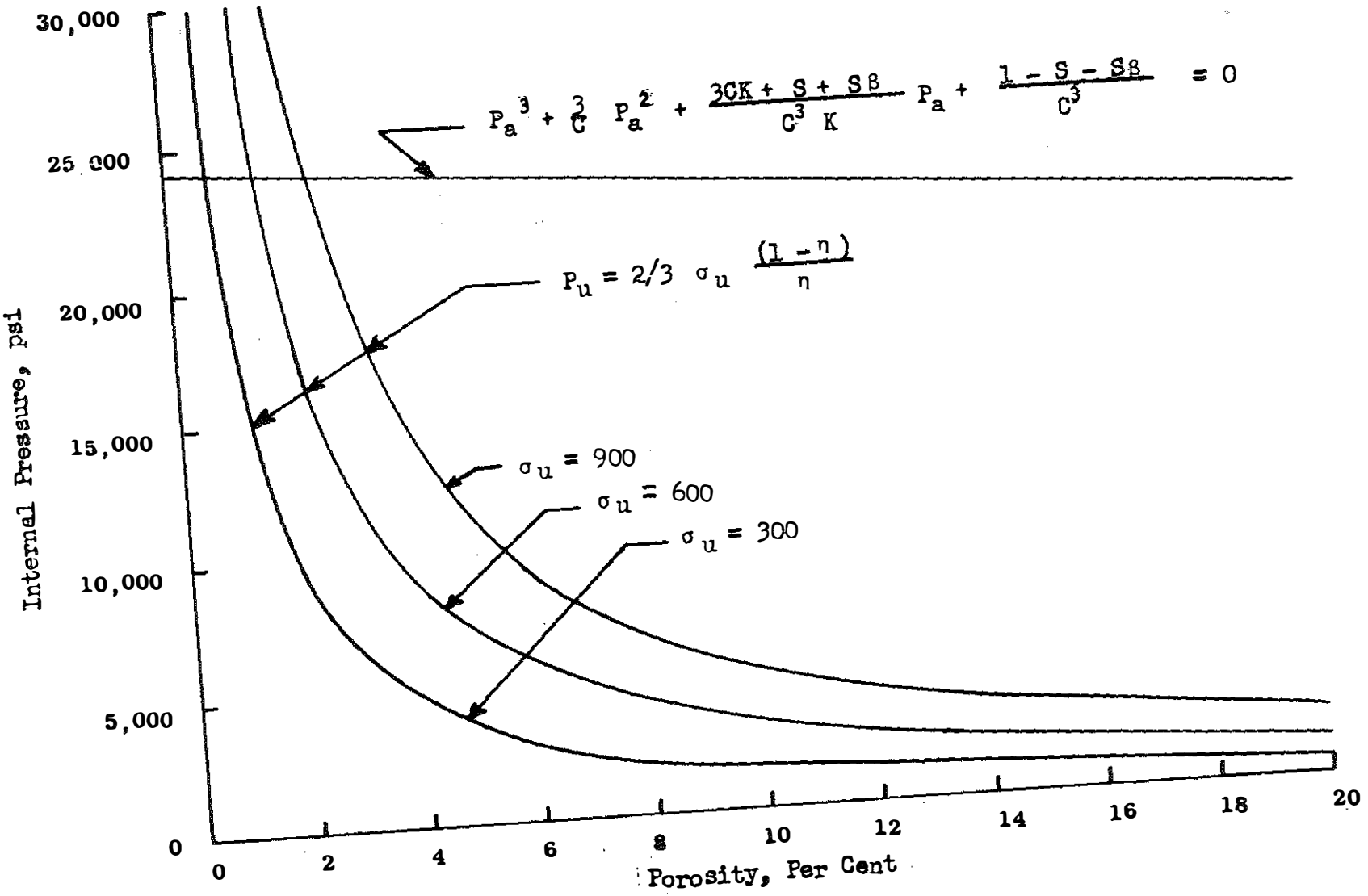

Figure 9: Suggested, Theoretical Relationship between Allowable Internal Pressure, P_u, and Available Internal Pressure, P_a, for Varying Porosities and Tensile Strengths.

$$\varepsilon_T = \frac{\delta}{R} = \frac{\sigma_T}{E} - \mu\frac{\sigma_T}{E} - \mu\frac{\sigma_R}{E}$$

where:

ε_T = tangential strain,

δ = radial displacement,

E = Young's modulus of elasticity, and

μ = Poisson's ratio.

Assuming $P_o = 0$, the increase in the radius of the internal cavity or void due to an internal pressure, P_a, is

$$\delta_a = \frac{(4\mu - 2)\ a^3 - (1 + \mu)\ b^3}{2E\ (a^3 - b^3)} \cdot aP_a$$

and, by multiplying and dividing the latter equation by $4/3\pi$ and substituting,

$$V_v = 4/3\pi a^3 = \eta V_t, \text{ and}$$
$$V_t = 4/3\pi b^3,$$

the equation reduces to

$$\delta_a = \frac{1+\mu+2\eta-4\mu\eta}{2E(1-\eta)} \cdot aP_a$$

The volume of the cavity, V_c, under internal pressure will, thus, be

$$V_c = 4/3\pi\ (a + \delta_a)^3$$

or

$$V_c = 4/3\pi\ a^3(C^3P_a{}^3 + 3C^2P_a{}^2 + 3C\ P_a + 1)$$

where:

$$C = \frac{1 + \mu + 2\eta - 4\mu\eta}{2E(1 - \eta)}$$

The volume of the ice within the cavity must be equal to the volume of the cavity and by equating the two, it follows that:

$$4/3\pi a^3 S(1 + \beta)(1 - \frac{P_a}{K}) = 4/3\pi a^3(C^3P_a{}^3 + 3C^2P_a{}^2 + 3C\ P_a + 1)$$

or

$$P_a{}^3 + \frac{3}{C}P_a{}^2 + \frac{3CK + S + S\beta}{C^3\ K}\ P_a + \frac{1 - S - S^\beta}{C^3} = 0$$

From the above relationship, it is seen that the respective dimensions disappear and that the internal pressure created by the freezing of water within a closed, spherical container is dependent upon the volume increase accompanying freezing of water, the bulk modulus of ice, and the porosity, degree of saturation, Poisson's ratio, and modulus of elasticity of the sphere.

The available internal pressure, P_a, was calculated for various porosity values by selecting, from the indicated references, the following values:

$\mu = 0.25$ (8),

$E = 2 \times 10^6$ psi (8),

$K = 0.392 \times 10^6$ psi (3),

$S = 1.00$, and

$\beta = 0.09$ (3).

This plot is superimposed on the maximum allowable internal pressure curves in Figure 9.

The intercept between the available-pressure curve and the appropriate allowable-pressure curve is the maximum allowable porosity value. For porosity values greater than this, the available pressure is greater than the allowable pressure and the container will rupture. Conversely, for porosity values less than this, the available pressure is less than the allowable pressure, and the container will withstand the pressure.

Critical porosity may be calculated by another method. An equation (10) expressing the force generated when particles are undergoing freezing, shows that the force developed is proportional to pore pressure, porosity and the effective spherical area encased within the ice shell. The equation is

$$F = P_p \times n \times a$$

where:

F = force in pounds,

P_p = pore pressure in psi,

n = porosity expressed as a decimal, and

a = effective area in $in.^2$

By arranging the equation so the porosity is the dependent variable, taking the maximum value for pore pressure (30,000 psi, -7.6°F), assuming a force of 600 pounds per unit area to equal the flexural strength of concrete, and taking the area of the sphere encased by the ice shell as unity, then the critical porosity is two per cent. If the flexural strength of the concrete is greater than 600 psi, then critical porosity increases; if the flexural strength is lower, then critical porosity decreases.

Applicability of Theory

The values of critical porosity obtained from the test data correspond closely to the theoretical values. It appears that the range over which critical porosity occurs is a manifestation of the inherent tensile strength of the aggregate. Whereas it must be presumed that tensile strength varies in inverse proportion to porosity, the inherent tensile strength varies

within a wide range depending on the mineralogical nature of the aggregate. Hence, the force opposing the expansion accompanying freezing--and therefore the limiting pressure--is governed by the restraining strength of the aggregate or the confining vessel. Logically, any encasement medium--such as mortar or concrete--will provide additional restraint against the forces emanating from a dilating particle of aggregate. Thus, restraint increases with depth of embedment. A saturated particle of aggregate in concrete may be viewed as being a center of compression, and the surrounding concrete may be viewed as a thick-walled shell or vessel. Of course, at near-surface locations, the restraint is unbalanced; and "pop-outs" or cracking will result if the dilating pressures are critical.

The pressures accompanying confined freezing cause an attendant depression of the freezing-point of the water--approximately 1750 psi per degree centigrade. Therefore, if the freezing-point of the water in an aggregate particle or in a cavity in concrete is monitored during a cooling cycle, the attendant active pressures may be deduced. To illustrate this mechanism, a small capsule of water was cast into a concrete block at a specific distance from the surface; a thermocouple was placed at the center of the sphere of water; and the block was frozen. A "pop-out"

resulted as shown in Figure 10. A typical thermogram is shown in Figure 11. There, the temperature at rupture is seen to be -4.2 degrees centigrade (7200 psi). Following rupture, the pressure subsided; and the freezing-point returned to normal. Thereafter the freezing was isothermal. This same type of thermogram has been obtained previously (4) by embedding thermocouples at the center of 6-in. by 6-in. cubes of concrete, but the events apparent in Figure 11 were displayed over a number of successive cycles rather than within a single temperature-excursion. This was interpreted to be a manifestation of progressive damage.

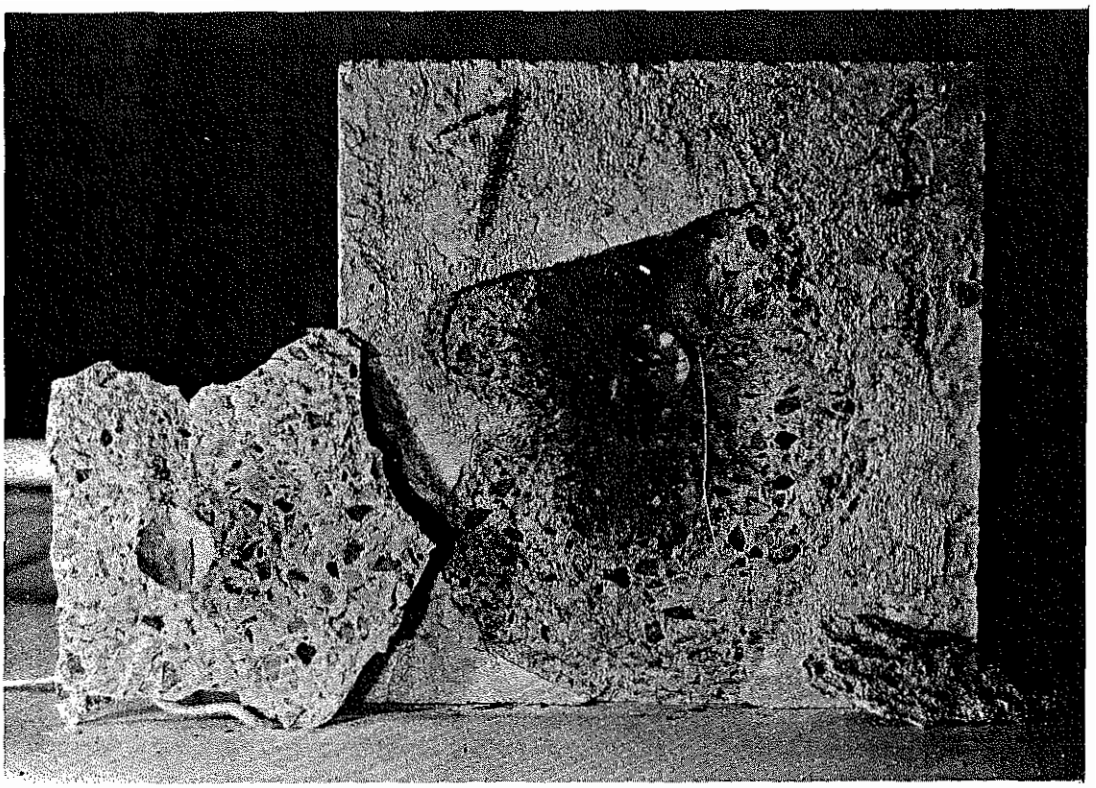

Figure 10: Concrete "Pop-out" Resulting from the Freezing of an Internal Sphere of Water.

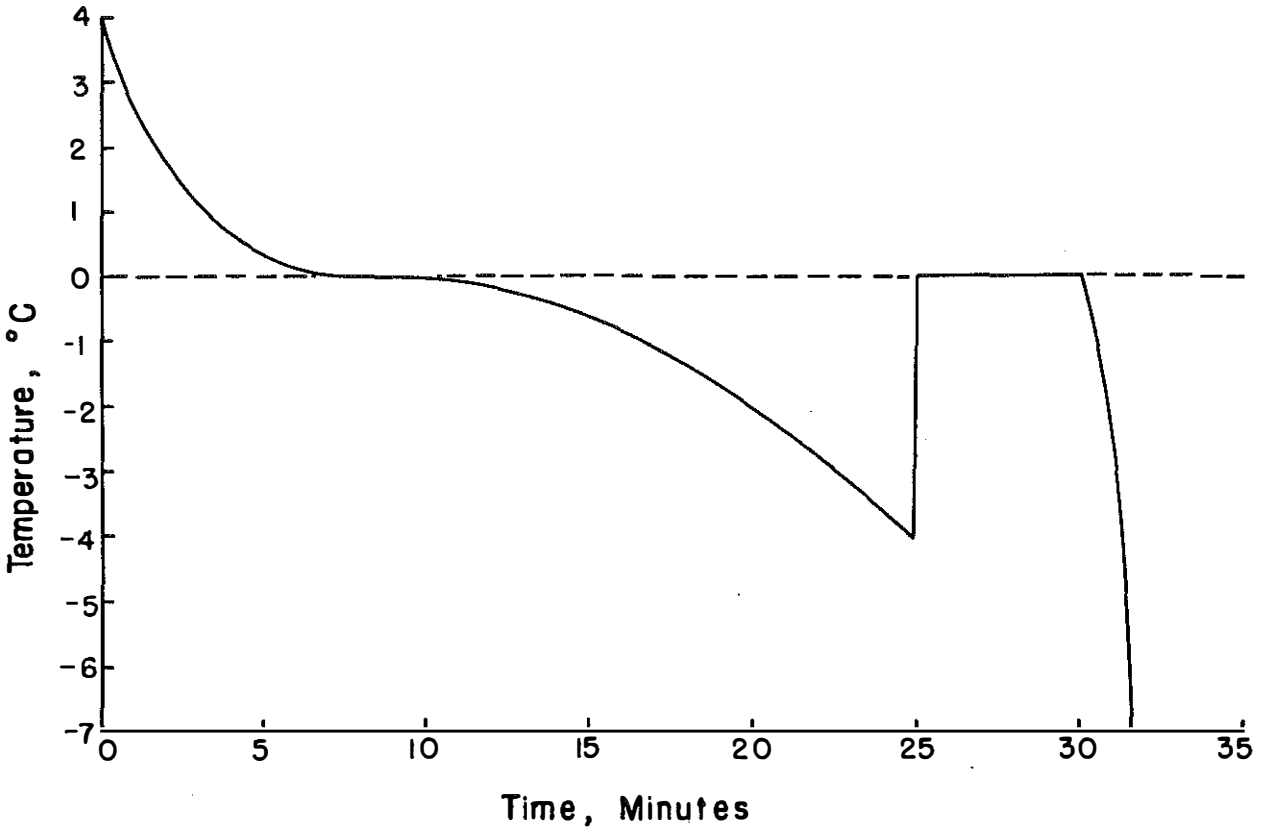

Figure 11: Typical Thermogram of a Sphere of Water Encased in Concrete Undergoing Freezing.

BIBLIOGRAPHY

1. Blanks, R. F., "Modern Concepts Applied to Concrete Aggregates," Proceedings, ASCE, Vol. 75, 1949.

2. Cantrill, C., and Campbell, L., "Selection of Aggregates for Concrete Pavement Based on Service Records," Proceedings, ASTM, Vol. 39, 1939.

3. Dorsey, N. E., Properties of Ordinary Water-Substance, Reinhold Publishing Co., New York, 1940.

4. Havens, J. H., "Thermal Analysis of the Freeze-Thaw Mechanism in Concrete," Bulletin No. 59, Engineering Experiment Station, College of Engineering, University of Kentucky, March, 1961.

5. Hodgman, Carles D. (ed.), Handbook of Chemistry and Physics, 39th ed., Chemical Rubber Publishing Co., Cleveland, 1958.

6. Jones, J. C., "The Relation of Hardness of Brick to Their Resistance to Frost," Transactions, American Ceramic Society, Vol. 9, 1907.

7. Klieger, P., "Effect of Entrained Air on Strength and Durability of Concrete Made with Various Maximum Sizes of Aggregate," Proceedings, Highway Research Board, Vol. 31, 1952.

8. Krynine, D. P., and Judd, W. R., Principals of Engineering Geology and Geotechnics, McGraw-Hill Book Co., Inc., New York, 1957.

9. Larson, T., Cody, P., Frazen, M., and Reed, J.; "A Critical Review of Literature Treating Methods of Identifying Aggregates Subject to Destructive Volume Changes when Frozen in Concrete and a Proposed Program of Research," Special Report 80, Highway Research Board, 1964.

10. Laughlin, G. R., (Unpublished).

11. Lemish, J., Rush, F. E., and Hiltrop, C. L., "Relationship of Physical Properties of Some Iowa Carbonate Aggregates to Durability of Concrete," Bulletin 196,

Highway Research Board, 1958.

12. Lewis, D. W., and Dolch, W. L., "Porosity and Absorption," Significance of Tests and Properties of Concrete and Concrete Aggregates, (Special Technical Publication, No. 169), ASTM, 1956.

13. Lewis, D. W., Dolch, W. L., and Woods, K. B., "Porosity Determinations and the Significance of Pore Characteristics of Aggregates," Proceedings, ASTM, Vol. 53, 1953.

14. Mitchell, Leonard J., "Thermal Expansion Tests on Aggregates, Neat Cements, and Concretes," Proceedings, ASTM, Vol. 53, 1953.

15. Powers, T. C., "Basic Considerations Pertaining to Freezing-and-Thawing Tests," Proceedings, ASTM, Vol. 55, 1955.

16. Powers, T. C., "Resistance to Weathering--Freezing and Thawing," Significance of Tests and Properties of Concrete and Concrete Aggregates, (Special Technical Publication, No. 169), ASTM, 1956.

17. Schuster, R. L., and McLaughlin, J. F., "A Study of Chert and Shale Gravel in Concrete," Bulletin 305, Highway Research Board, 1961.

18. Scott, J. W. and Laughlin, G. R., "A Study of the Effects of Quick Freezing on Saturated Fragments of Rocks," Research Division, Kentucky Department of Highways, February, 1964, (unpublished).

19. Sweet, H. S., "Chert as a Deleterious Constituent in Indiana Aggregates," Proceedings, Highway Research Board, Vol. 20, 1940.

20. Sweet, H. S., "Research on Concrete Durability as Affected by Coarse Aggregates," Proceedings, ASTM, Vol. 48, 1948.

21. Sweet, H. S., and Woods, K. B., "A Study of Chert as a Deleterious Constituent in Aggregates," Research Series 86, Engineering Bulletin of Purdue University, September, 1942.

22. Thomas, W. N., "Experiments on the Freezing of Certain Building Materials," Building Research Technical Paper No. 17, Department of Scientific and Industrial Research, England, 1938.

23. Timoshenko, S., Theory of Elasticity, McGraw-Hill Book Co., Inc., New York, 1934.

24. Walker, R. D., and McLaughlin, J. F., "Effect of Heavy Media Separation on Durability of Concrete Made with Indiana Gravels," Bulletin 143, Highway Research Board, 1956.

25. Wray, F. N., and Lichtefeld, H., "The Influence of Test Methods on Moisture Absorption and Resistance of Coarse Aggregate to Freezing and Thawing," Proceedings, ASTM, Vol. 40, 1940.

26. Wuerpel, C. E., and Rexford, E. P., "The Soundness of Chert as Measured by Bulk Specific Gravity and Absorption," Proceedings, ASTM, Vol. 40, 1940.